EPOXY-GRAPHENE UV-CURED NANOCOMPOSITES

M. Sangermano[1], M. Martin-Gallego[2], R. Verdejo[2] M.A. Lopez-Manchado[2]

[1]*Politecnico di Torino, Dipartimento di Scienza Applicata e Tecnologia, C.so Duca degli Abruzzi 24, 10129, Torino.*
[2]*Instituto de Ciencia y Tecnología de Polímeros, CSIC, Juan de la Cierva, 3 28006-Madrid, Spain.*

INTRODUCTION

Graphene is considered a two-dimensional carbon nanofiller with a one-atom-thick planar sheet of sp^2 bonded carbon atoms that are densely packed in a honeycomb crystal lattice [1,2]. Graphene is predicted to have remarkable performance, such as high thermal conductivity, excellent electronic transport properties and superior mechanical properties[3-6]. In fact graphene sheets were demonstrated to have extraordinary electronic transport properties[7], combined with a wide set of other unusual properties[8]: their thermal conductivity and mechanical stiffness may rival the remarkable in-plane values for graphite (3,000Wm^{-1}K^{-1} and 1,060 GPa, respectively). Of particular interest is the fact that their fracture strength should be comparable to that of carbon nanotubes (CNT) for similar types of defects[9-11]. Therefore, the tensile strength of graphene is similar or slightly higher than CNT, but much higher than steel and Kevlar. Besides they should show a good electrical properties which could deeply modify the conductivity of the polymeric matrix.

The superior properties of graphene are also reflected in polymer/graphene nanocomposites, and it is evident that the transfer of such features to polymeric materials usable at the application level, holds a deep scientific interest. Novel graphene-based polymer composites are presently emerging as a new class of highly functional advanced materials that hold promise for a more versatile and cheaper alternative to carbon nanotubes-based composites. In fact, while the addition of carbon nanotubes to polymer matrices has already been shown to improve mechanical, electrical and thermal properties[12], the challenge is now to exfoliate the graphite to single graphene sheets to be used as an inexpensive and feasible substitute to carbon nanotubes. These nanohybrid materials could show considerable improvement in properties that cannot normally be achieved using conventional composites or virgin polymers. In particular, polymer/graphene nanocomposites show superior, thermal, gas barrier, electrical, flame retardant and mechanical properties compared to the neat polymer[13-15]. It was reported that the improvement in mechanical and electrical properties of graphene based polymer nanocomposites are much better in comparison to that of other carbon filler-based polymer nanocomposites. Despite the promising applications of graphene in epoxy UV-curable resins, to the best of our knowledge no reports are present in literature so far. Therefore, this paper intend to investigate the effect of graphene on the UV-curing process of an epoxy resin by evaluating the photopolymerization kinetics in real-time and the final thermal viscoelastic properties and electrical properties of the cured materials.

EXPERIMENTAL

Materials

Bis-cycloaliphatic diepoxy resin 3,4-epoxycyclohexylmethyl-3',4'-epoxycyclohexyl carboxylate, (CE), triphenylsulfonium hexafluoroantimonate (Ph$_3$S$^+$SbF$_6$$^-$) were purchased from Sigma-Aldrich (Milan, Italy) and used as received without any further purification. Functionalized graphene sheets (FGS) were synthesized as previously reported [25].

Sample preparation

Graphene was directly dispersed in the range between 0.5 to 1.5 wt% in the epoxy resin by means of Ultraturrax, a mixing procedure at 30000 rpm for 10 minutes and 10 minutes in an ultrasonic bath was carried out to reach a good dispersion of the carbon filler in the resin. After mixing, 2 wt% photo-initiator (triphenylsulfonium hexafluoroantimonate) was added to each formulation. To prepare the DMTA and surface hardness test samples, the formulations were coated on glass substrates and cured with UV-light. The UV-induced polymerization was promoted by UV irradiation (UV lamp Italyquartz, Milano, Italy), with a light intensity on the surface of the sample of about 55 mW/cm^2 during 15 minutes (7.5 minutes each side of the sample) while 3 minutes were applied to the transparent pristine epoxy resin. Homogeneously UV-cured films of about 150 μm in thickness and 25 mm in length and 3 mm width were produced.

Sample characterization

The extent of the photo-polymerization reaction was determined by Real-Time-FTIR spectroscopy (RT-FTIR, using the instrument Thermo-Nicolet 5700). 25 μm-thick formulations were coated onto silicon wafers and simultaneously exposed to the UV beam (HAMAMATSU LC8) with an intensity of 35 mW/cm^2, to induce polymerization, and to the IR beam, to make an in-situ evaluation of the extent of reaction. Epoxy groups conversion was followed by monitoring the decrease in the absorbance of the epoxy groups centered at 750 cm^{-1} and normalized with the carbonyl peak centred at around 1700 cm^{-1}. The conversion of the cured samples used for the thermal and viscoelastic characterization was determined by carrying out a single spectrum after 5 minutes of irradiation with the UV lamp at a light intensity of 55 mW/cm^2 on a coated film of about 25 μm.

The gel content was determined on the cured films by measuring the weight loss after 24 h extraction with chloroform at room temperature, according to the standard test method ASTM D2765-84.

The morphological characterizations of the cured films were performed by Scanning Field Emission Scanning Electron Microscopy (FESEM, Zeiss Supra 40) at 350 kV. All the samples were cryo-fractured in liquid nitrogen and the fracture surface was sputter coated with gold/palladium (Au/Pd 80/20). The study of the dispersion of the graphene was also carried out using transmission electron microscopy (TEM Leo 910 microscope at an acceleration voltage of 80 kV). Ultra-thin sections of the samples were prepared by cryo-ultramicrotomy at -140 ºC (Leica EM UC6).

Dynamic-mechanical thermal analysis (DMTA) was performed on a MK III Rheometrics Scientific Instrument at 1 Hz frequency in the tensile configuration. The storage modulus, *E'*, and the loss factor, *tan δ*, were measured from 0 °C up to the temperature at which the rubbery state was attained. The T_g value was assumed as the maximum of the loss factor curve (*tanδ*).

DSC measurements were performed under nitrogen flux of 2 ml/min, in the range of 25 °C to 250 °C with a heating rate of 20 °C/min, with a Mettler TC 10A/TC15 TA controller instrument.

The pendulum hardness (Persoz, ASTM D4366) was measured from the damping of the oscillation of the pendulum. Pendulum hardness values are expressed in number of pendulum oscillations and are related directly to the softness of the surface of the sample. The shorter the damping time, the lower is the hardness.

The nanohardness of the coatings was measured by depth-sensing Berkovich nanoindentation (Nano-Indentation Tester, CSM Instruments) on the surface of plain coated samples. The maximum load was fixed at 50 mN (5 indentations per sample, loading/unloading rate of 40mN/min), corresponding to a maximum indentation depth ≤ 10% of the thickness of each tested coating, so that the nano-hardness values are representative of the intrinsic properties of the film itself.

Broadband dielectric spectroscopy was performed on an ALPHA high-resolution dielectric analyser (Novocontrol Technologies GmbH, Hundsangen, Germany). The photocured films were held in the dielectric cell between two parallel gold-plated electrodes. The dielectric response of each sample was assessed by measuring the complex permittivity $\varepsilon^*(\omega) = \varepsilon'(\omega) - j\varepsilon''(\omega)$ over a frequency range

window of 10^1 to 10^7 Hz at room temperature. The amplitude of the alternating electric current applied to the samples was 1 V.

RESULTS AND DISCUSSION

UV-Curing process

The aim of this study was the preparation and characterization of graphene/epoxy coatings cured by cationic photopolymerization processing. The effect of the graphene on the UV-curing process was evaluated by RT-FTIR analysis. Figure 1a shows representative FTIR spectra as a function of time for both pristine and 1.5 wt% FGS filled samples. The decrease of the epoxy group band, centered around 750 cm^{-1}, as a function of irradiation time provides an indication of the extent of the reaction. Hence, the conversion curves of all samples were calculated from the normalized absorbance of the epoxy by the carbonyl band (Figure 1b). From the slope of the RT-FTIR kinetic curves it is easy to evaluate the rate of polymerization (Rp) which can be calculated at any moment of the reaction; the plateau value gives the final epoxy group conversion

Figure 1a: FT-IR spectra in the region between 950-650 cm^{-1} for the neat epoxy and the formulation containing 1.5% FGS. Light intensity on the surface of the sample 35mW/cm^2. Film thickness 25 μm.

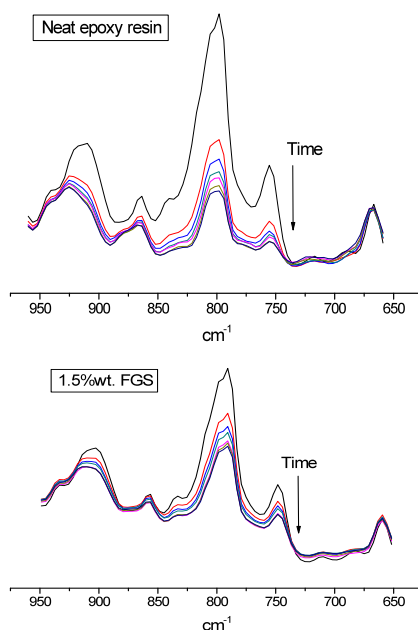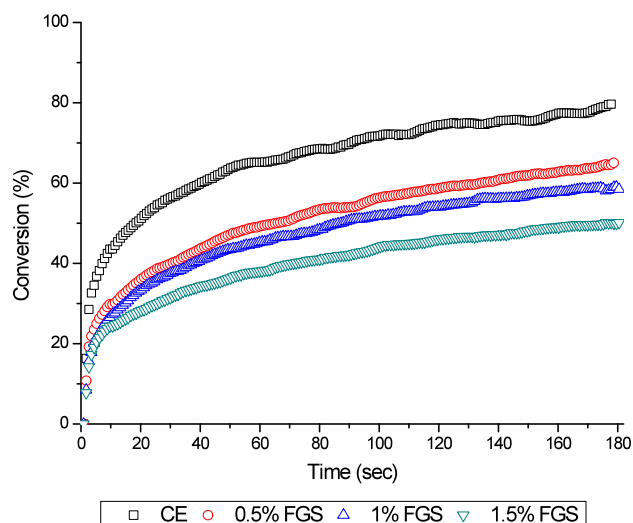*Figure 1b: Real-time FTIR conversion curves as a function of irradiation time for the pristine CE resin (□) and for the epoxy resin formulations containing 0.5 (○), 1 (△) and 1.5 (▽) wt% of the graphene. Light intensity on the surface of the sample 35mW/cm². Film thickness 25 μm.*


From the curves reported in Figure 1, it is evident the high reactivity of the epoxy groups of the CE resin with a quite high initial rate of polymerization. The epoxy group conversion levels off, after 3 minutes of irradiation, to a value of about 80%. This is due to the formation of a glassy polymer network, which hindered the mobility of the reactive species so that a large number of unreacted epoxy groups remained trapped within the glassy polymer network.

The addition of graphene to the photocurable formulations led to a decrease of both the polymerization rate and the final conversion as a function of loading fraction. The epoxy group conversion decreased to a minimum of 50% at 1.5 wt.-% FGS content. Meanwhile, the curing rates of filled samples were slightly lowered than the unfilled system. The relatively lower rate of conversion, which can be put in evidence only by using a lower irradiation intensity, may be due to the UV light shielding effect of graphene: a lower amount of reactive species is photogenerated resulting in a decrease of the epoxy group conversion. In fact, the efficiency of the photo-initiation process can be described by two quantum yields: the *quantum yields of initiation*, which represents the number of starting polymer chains per photons absorbed, and the *quantum yields of polymerization*, which is the number of monomer units polymerized per photons absorbed. Therefore, it is clear that the competition in absorption with the carbon filler implies a decrease of the photons absorbed by the photo-initiator. This can lead to a decrease of quantum yields and therefore to a lower epoxy group conversion. A similar behavior was previously observed when CNTs were dispersed into UV-curable epoxy resin[16].

In order to overcome this shielding effect, the formulations were cured for 5 minutes at 55 mW/cm². By increasing irradiation time and light intensity we could achieve fully cured networks. In Figure 2 the FT-IR spectra, in the region between 950-650 cm⁻¹, are reported for the epoxy formulation containing 0.5% of FGS before and after 5 minutes of UV irradiation. It is possible to observe the almost complete disappearance of the epoxy group band centered at around 750 cm⁻¹. All the cured samples showed a high gel content value (above 99%, see Table 1), showing the absence of any extractable oligomer or unreacted monomer.

Figure 2: IR spectra of the formulation containing 0.5% FGS before a) and after 5 minutes of UV irradiation b). Film thickness 25 μm.
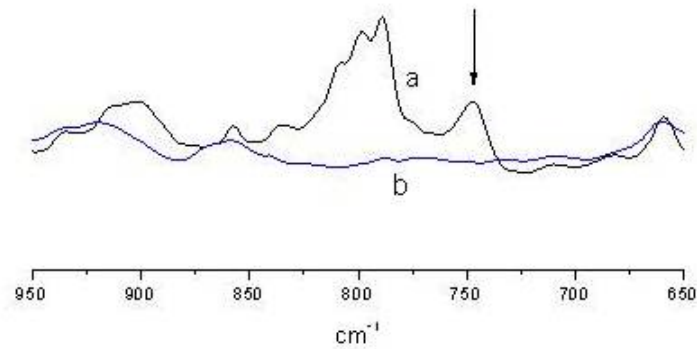
## Morphological investigation

The morphology of the UV-cured hybrid materials was investigated by FESEM observations on the cross-sections of the films. In Figure 3 high magnification FESEM micrographs are reported for the cured epoxy resin and for the formulation containing 1.5 wt% of graphene. Figure 3a show a typical fragile behaviour of epoxy matrices, whereas a less brittle-like fracture is observed for the nanocomposite sample in figure 3b.

Figure 3: FE-SEM images obtained on the fracture surface of the cured samples. Pristine epoxy resin a) and nanocomposite film containing 1.5 wt% of graphene filler b).
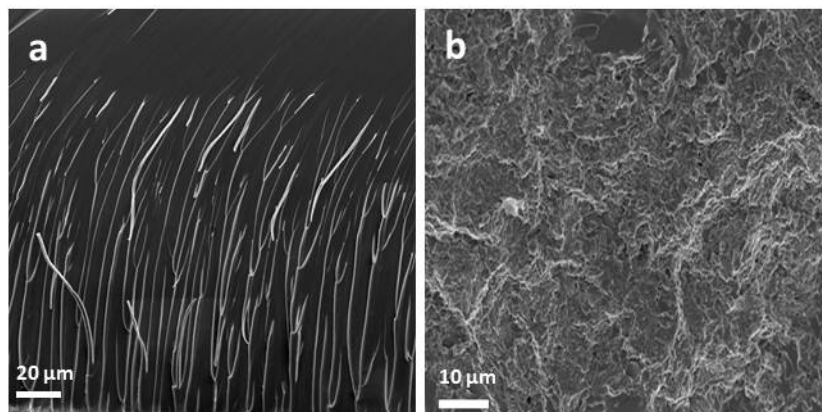
TEM images of the CE/graphene composites (Figure 4) show that single graphenes or stacks of graphene with thicknesses of several nanometers were uniformly dispersed throughout the polymer matrix. The particles appear to be completely embedded in the epoxy resin indicating an intercalated structure. This reflects a good compatibility between the graphene and epoxy resin without additional surface treatment.

Figure 4. TEM images of graphene-epoxy resin composite at a 1.5 wt% of filler.
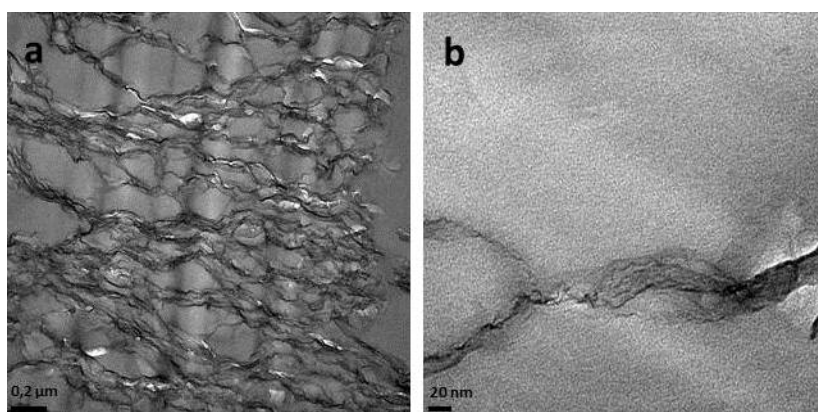
Thermal and Viscoelastic characterization

Thermal and dynamic-mechanical analysis were performed on the cured films. While DSC analysis gives information about the thermal behaviour, DMTA analysis allows the evaluation for the elastic and viscous components of the modulus of the material over a large temperature range. Therefore, these techniques give a complete characterization of the thermal and viscoelastic properties of the material. Firstly, the T_g values of UV-cured films were evaluated by means of DSC analysis. It was possible to observe a strong increase of the T_g value as a function of the graphene content in the UV-curable formulations (see Table 1). The T_g increase could be due to the constraint effect of graphene sheets on the polymer chain mobility. This results suggest a uniform and homogeneous distribution of the graphene platelets within the polymeric network. In order to analyze this behavior, a further detailed study about the effect of graphene on the molecular dynamic of epoxy resin by dielectric spectroscopy will be carried out.

Viscoelastic characterization of the cured films was evaluated by DMTA analysis. CE resin shows a main relaxation process α assigned to the glass transition temperature (see Figure 5). This relaxation is gradually shifted towards higher temperatures with increasing graphene content in the composite. The T_g values taken as the maximum of the $tan\delta$ curves display the same upward trend than those previously determined by DSC (Table 1). It can be observed, anyway, that the T_g values obtained by DMTA are higher than those obtained by DSC; this is a general behavior previously observed and it was attributed to a frequency effect[17].

Table 1: Properties of UV-cured epoxy films obtained in the presence of graphene filler.

Sample	Conv. [%][1]	Conv. [%][2]	Gel content [%][3]	T_g [°C][4]	T_g [°C][5]
CE	80	100	100	155	206
0,5% FGS	65	100	100	167	214
1% FGS	59	95	100	181	230
1,5% FGS	50	98	99	195	243

1: plateau values of the RT-FTIR conversion curves as a function of irradiation time (UV intensity of 35 mW/cm^2)
2: determined by the single spectra taken before and after 5 min of UV irradiation (UV intensity of 55 mW/cm^2)
3: determined gravimetrically ASTM D2765-84
4: determined by DSC analysis, scan-rate 20 °C/min
5: determined by DMTA analysis, tensile configuration, 1 Hz frequency

Plots of the storage modulus versus temperature (Figure 6) allow a direct comparison of the different UV cured networks. Graphene addition to the epoxy UV-curable system induces an increase of the storage modulus and, more important, of the viscoelastic properties by extending the performance of the storage modulus to higher temperatures. The viscoelastic transition, seen as the decrease of the modulus, is shifted to higher temperature by increasing the graphene content in the photocurable formulations. It has been already suggested that the observed mechanical reinforcement may be related to the graphene high specific surface area, the enhanced nanofiller-matrix adhesion/interlocking arising from their rough surface, as well as the two dimensional planar geometry of the graphene platelets. This is a remarkable result, since it clearly highlights the important increase on mechanical performance achieved for the hybrid films probably due to the interaction between the polymeric chains and the graphene platelets, with a consequent increase on stiffness and T_g values.

These features can be accompanied by an increase on surface hardness. Therefore we investigated the surface hardness of cured films by means of Persoz pendulum and nano-indentation measurements. Figure 7 shows the surface hardness values measured by the Persoz pendulum and nano-indentation tests as a function of filler content. Persoz pendulum shows a clear increase of the cycles with FGS content. This hardness increase can be related to the hindering effect of the polymer chain mobility induced by the graphene platelets dispersed within the polymeric matrix. This result was also observed by the nano-indentation tests, since they both follow the same trend. However, the results obtained by nano-indentation have large standard deviation errors that should be taken into consideration.

Figure 5: Tanδ curves obtained by DMTA analysis for epoxy UV cured system and its graphene composites.
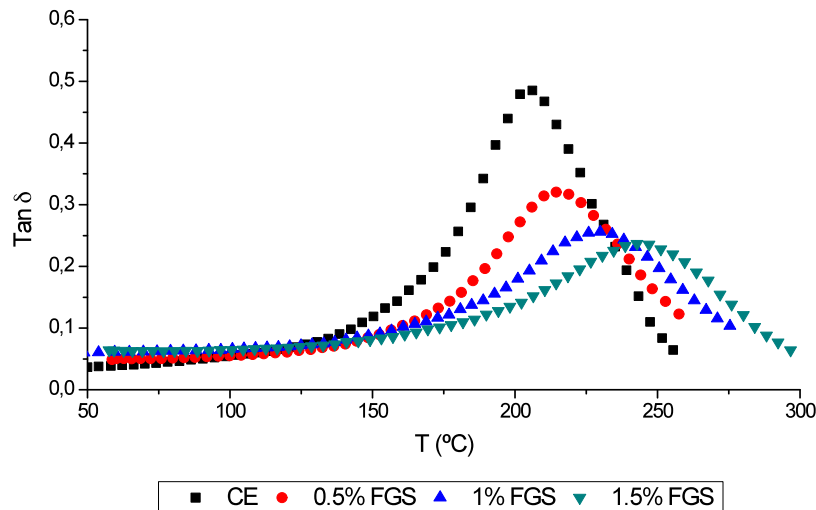
Figure 6: Storage modulus curves obtained by DMTA analysis for epoxy UV cured system and its graphene composites.
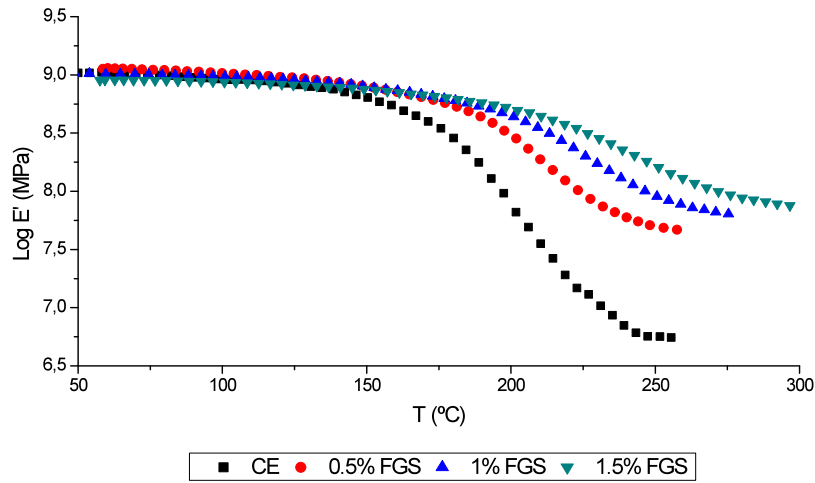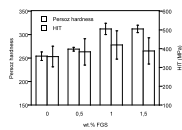

Figure 7: Number of oscillations of the Persoz pendulum and surface modulus (HIT) determined by nano-indentation test of cured films as a function of graphene content.

Dielectric properties

The dielectric properties of the photocured epoxy nanocomposites at different nanofiller contents measured at room temperature are depicted in Figure 8. The electrical conductivity and dielectric permittivity were significantly increased by the addition of nanofillers. The conductivity with just a small percentage of filler became independent of the frequency in almost all the range of study. While the dielectric permittivity had the opposite behaviour, passing from being independent of the frequency to reveal a negative slope when the concentration was above the percolation threshold due to polarizarion effects between clusters inside the percolated system, the antistatic limit of 10^{-8} S/cm is reached.

Figure 8: AC conductivity and permitivity versus frequency for at different loading fractions.
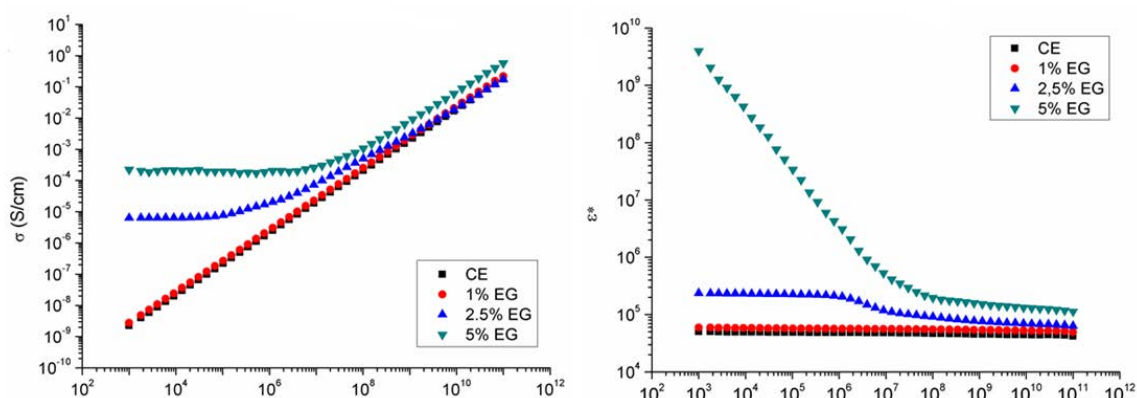
REFERENCES

1. Novoselov KS, Geim AK, Morozov SV, Jiang D, Zhang Y, Dubonos SV, Grigorieva IV, Firsov AA. Science 2004;306:666-669.
2. Novoselov KS, Geim AK, Morozov SV, Jiang D, Katsnelson MI., Grigorieva IV, Dubonos SV, Firsov AA. Nature 2005;438:197-200.
3. Wang G, Yang J, Park J, Gou X, Wang B, Liu H, Yano J. J. Phys. Chem. C 2008;112:8192–8195. Wang G, Shen X, Wang B, Yao J, Park J. Carbon 2009;47:1359–1364.
4. Li X, Wang X, Zhang L, Lee S, Dai H. Science 2008;319:1229–1231.
5. Blake P, Brimicombe PD, Nair RR, Booth TJ, Jiang D, Schedin F, Ponomarenko LA, Morozov SV, Gleeson HF, Hill EW, Geim AK, Novoselov KS. Nano Lett. 2008;8:1704–1708.
6. Berger C, Song Z, Li T, Li X, Ogbazghi AY, Feng R, Dai Z, Marchenkov AN, Conrad EH, First PN, de Heer WA. J. Phys. Chem. B 2004;108:19912-19916
7. Stankovich S, Dikin DA, Dommett GHB, Kohlhaas KM, E. J. Zimney EJ, Stach EA, Piner RD, T. Nguyen ST, Ruoff RS. Nature 2006;442:282-286.
8. Dresselhaus MS, Dresselhaus G, Adv. Phys. 2002;51:1-186.
9. Hirata M, Gotou T, Horiuchi S, Fujiwara M, Ohba M. Carbon 2004;42:2929-2937.
10. Yu MF, Lourie O, Moloni K, Kelly TF, Ruoff RS, Science 2000;287:637-640.
11. Shafer MS, Sandler J, In: "Carbon nanotube/nanofiber polymer composites", S. Advani Ed., World Scientific, 2006, pp. 1-59.
12. Eda G, Chhowalla M. Nano Lett. 2009;9:814–8.
13. Liang J, Xu Y, Huang Y, Zhang L, Wang Y, Ma Y, Li F, Guo T, Chen Y. J. Phys. Chem. C 2009;113:9921–9927.
14. Kim H, Macosko CW. Polymer 2009;50:3797–3809.
15. Sangermano M, Pegel S, Potschke P, Voit B. Macromol. Rapid Commun. 2008;29:396-400.
16. Nielsen LE, "Mechanical Properties of Polymers and Composites", New York, Dekker, 1994.